

1 of 1

10
4-4-94 JSD ①

Conf-930855--9

SLAC-PUB-6320
SLAC/SSRL-0049
August 1993
(SSRL-M)

SELECTED APPLICATIONS OF PLANAR PERMANENT MAGNET MULTIPOLES IN FEL INSERTION DEVICE DESIGN*

Roman Tatchyn

Stanford Linear Accelerator Center, Stanford Synchrotron Radiation Laboratory,
Stanford University, Stanford, California, 94309

Abstract

In recent work, a new class of magnetic multipoles based on planar configurations of permanent magnet (PM) material has been developed. These structures, in particular the quadrupole and sextupole, feature fully open horizontal apertures, and are comparable in effectiveness to conventional iron multipole structures. In this paper results of recent measurements of planar PM quadrupoles and sextupoles are reported and selected applications to FEL insertion device design are considered.

Presented at the 15th International Free Electron Laser Conference,
The Hague, The Netherlands, August 23-27, 1993

* Supported by DOE Offices of Basic Energy Sciences and High Energy and Nuclear Physics and Department of Energy Contract DE-AC03-76SF0015

1. Introduction

Conventional multipole (N-pole) field generators typically consist of N-fold rotationally symmetric iron yokes excited by current windings. Permanent magnet structures with the same general symmetry and similar material or field distributions have also been designed [1] and employed. Due to the emphasis on maximal rotational symmetry, the field distributions of such structures at relatively large distances from the symmetry axis remain dominated by their leading multipole components. This can be advantageous, for example, in the analysis or design of complex focusing lattices with large dynamic apertures. Notwithstanding this, structures that completely enclose the particle axis can sometimes present impediments to effective lattice design and operation. Two examples include: 1) the implementation of focusing lattices in small gaps; and 2) the inhibition of lateral access to the particle beam for diagnostic purposes. In recent work, for example, both situations were encountered in the design of a 1.5cm gap, 60m long permanent magnet (PM) undulator for the proposed 4nm FEL project at SLAC [2]. Due to the anticipated sub-100 μ levels of beam size and drift in this device, an alternative, less symmetric configuration for the usual focusing quadrupole [3] was proposed (see Fig. 1(left)). Apart from the unconventional field distribution, a number of potentially advantageous features are also apparent. These include: 1) a fully open horizontal aperture; 2) a low net vertical profile; 3) maximal ease of fabrication and magnetization; 4) flexible design and implementation of focusing (e.g., FODO) lattices; and 5) the possible attainment of large focusing gradients with small amounts of PM material. In subsequent work, the notion of the planar PM quadrupole has been extended to sextupoles and higher order multipoles [4]. A schematic front view of an arbitrarily configured sextupole is shown in Fig. 1 (right).

Due to the compactness and simplicity of these elements, a number of novel control and design options suggest themselves [3]. For example, a method for tuning their fields with external permeable sheets has been considered (see Fig. 2). More generally, it can be shown that replacing the (plane) sheets with more arbitrary permeable material distributions possessing left-right symmetry will also modulate the free-space components without introducing any new ones. In configuring focusing (e.g., FODO) lattices, this important property allows the installation of planar PM elements into the gaps of different classes of undulators: pure-PM, hybrid, PM-free electromagnetic, iron-free electromagnetic, and others, including devices with non-magnetic fields. In undulators with permeable poles, the shapes and permeabilities of the pole surfaces must exhibit the appropriate left-right symmetry. When the undulator and focusing lattice are both pure PM, it becomes possible to consider tuning the undulator field by the method of induced images, a potentially attractive option for (sub-octave) tuning of ultra-long undulators

MASTER

REPRODUCTION OF THIS DOCUMENT IS UNLAWFUL EP

in which jaw motion is impracticable. More generally, the planar PM multipoles promise an increased design flexibility for controlling the spectral and particle-focusing properties of insertion devices.

In this paper measurements of recently fabricated planar PM quadrupoles (quads) and sextupoles are reviewed [5] and possible applications to the design of FEL insertion devices are discussed.

2. Field distributions

The potential of each of the structures in Fig. 2 can be expanded about $x=y=0$ in a real Taylor series whose terms can be associated with the field multipole components [4]. For the PM quadrupole, we have

$$\phi_Q(x, y) = C_{11}xy + E_{13}(xy^3 - x^3y) + \dots, \quad (1)$$

with

$$C_{11} = \frac{-2B_r}{\pi} \left[\frac{w^2}{g'(w^2 + g'^2)} \right]_{g'=h+(g/2)}^{g'=(g/2)}, \quad (2)$$

where $B_r[T]$ is the PM's remanent field. Evidently, the field gradients are given by

$$\frac{\partial B_x(x, y, 0)}{\partial y} = \frac{\partial B_y(x, y, 0)}{\partial x} = C_{11} + 3E_{13}(y^2 - x^2) + \dots, \quad (3)$$

where C_{11} represents the dominant quadrupole field component, and the next term describes the (antisymmetric in x vs y) octupole component. The variable terms indicate that the planar PM quadrupole will closely approximate an ideal quadrupole in regions sufficiently close to the axis (viz., for values of (x, y) for which the term containing E_{13} remains substantially smaller than C_{11}).

In the analogous expansion of the sextupole, the leading term represents a dipole component. Thus,

$$\phi_S = B_{01}y + D_{21}(3x^2y - y^3) + F_{41}(5x^4y - 10x^2y^3 + y^5) + \dots, \quad (4)$$

with

$$D_{21} = \frac{2B_r}{3\pi} \left[\frac{2g'b}{(a^2 + g'^2)^2} - \frac{ag'}{(b^2 + g'^2)^2} \right]_{g'=h+(g/2)}^{g'=(g/2)}. \quad (5)$$

Evidently, to create a field with a leading sextupole component, the condition $B_{01}=0$ must be satisfied.

3. Measurement apparatus and stand-alone PM multipole test results

A rotating-coil probe was prepared for the multipole tests. It consists of a rectangular 2mm x 1cm coil with one of its long sides set on the multipole symmetry axis. The outer side consequently rotates on a cylindrical surface with an average 2mm radius. At a rotation frequency of 30 Hz, a harmonic decomposition of the signal reveals the fundamental quadrupole component and the higher components along the 2mm circumference of rotation. The magnitudes of the field components are unfolded from the rotation rate and a knowledge of the coil's geometry and electrical parameters.

A number of planar PM multipoles were designed at SSRL and the individual rectangular pieces fabricated by Magnet Sales and Manufacturing, Inc. [6]. The geometric and field parameters of two of the samples are listed in Table 1. Front views of the experimental configurations for measuring the PM quadrupole and sextupole fields with steel image plates are schematized in Fig. 2.

A typical rotating-coil spectrum is shown in Fig. 3. The calculated vs measured field components are listed in Table 2. The calculated values in the table have been scaled to establish agreement between the measured and calculated dominant field components in the "free-space" cases. The remanent fields, unfolded from the measured and scaled field components, are presumed to represent the actual magnetization fields. With regard to the experimental errors and scaling, the measured field components agree closely with free-space and image-tuning calculations based on equ's. (1-5). Other samples (configured out of SmCo) exhibited greater discrepancies, which are presently being further investigated.

4. Tests of a PM quadrupole installed in a prototype PALADIN section

A potentially important application of the planar PM multipoles is to configure superimposed focusing or aberration-correcting fields over the primary fields of insertion devices or other machine elements. In FEL insertion devices, enhanced focusing can significantly improve the attainable gain for a given undulator length [7]. For example, recent investigations by the SLAC FEL research group [8] have indicated that increasing the K value and focusing strength of the PALADIN [9] undulator would make it possible to reduce the wavelength at which SASE saturation (in the available 25m length) could be attained from 120nm down to about 40nm. With this and similar applications in mind, the feasibility of installing and operating a PM planar quadrupole in the aperture of a prototype section of PALADIN was investigated. PALADIN's existing sextupole focusing [10] is determined by the gap and geometry of the concave cutouts in its pole faces. As indicated in Fig. 4, the aperture provided by these cutouts allows sufficient room to install a relatively strong-field planar PM quadrupole with a resulting vertical 1cm gap. In our initial characterization, we: 1) measured the B_y field component in the x -direction with no quadrupole

in the aperture and the peak field amplitude set to about 0.5T; 2) installed a NdFe/B quadrupole (Sample 1) into PALADIN's gap on a specially prepared brass support and took a scan of its field in the x direction with the prototype's field turned off; and 3) took the same x-scan with the field turned back to 0.5T. These results are presented in Fig. 5. Numerical analysis of the different curves indicates that, to within about 1%, the fields of PALADIN and the 57T/m PM quadrupole superpose linearly. The magnitude of this discrepancy can be fully accounted for by systematic experimental errors stemming from torque-induced misalignments. Effects related to the asymmetric (left-right) interaction of the poles' and quad's fields with the yoke poles running in a non-linear permeability regime could also account for some part of the discrepancy, although in the present case this effect is estimated to be small.

5. Discussion

Given the wide value ranges of the planar PM multipole parameters, the experimental work reported here indicates that enhanced flexibility in the design of focusing or aberration-correcting components and lattices with sub-centimeter gaps and 100+T/m gradients (in a quadrupole lattice) can be achieved.

With regard to focusing in FEL insertion devices, a systematic 1-D analysis of the dependence of the ρ parameter on the lattice β [11] is easily performed [12]. For a helical undulator, we have

$$\rho = \gamma^{-1} \left(5.6 \times 10^{-15} K^2 n_e \lambda_u^2 \right)^{\frac{1}{3}}, \quad (7)$$

with $K (=0.934 \lambda_u [\text{cm}] B_0 [\text{T}])$ the undulator parameter, n_e [#/cm-] the bunch particle density, B_0 the undulator field amplitude, and λ_u the undulator period. To explicitly query β , we employ the substitutions $n_e = I_p / 2\pi c q \epsilon \beta$, $\lambda_u = 2\gamma^2 \lambda / (1 + K^2)$, and $\beta^{-2} = \beta_u^{-2} + \beta_{ext}^{-2}$. Here I_p is the peak current, ϵ is the beam emittance, λ is the output wavelength, and β is expressed in terms of the natural undulator beta, $\beta_u (= \gamma \lambda_u / \pi K)$, and an independent, external beta, β_{ext} . For operation at $\epsilon = \lambda / 2\pi$, eq. (7) becomes

$$\rho = \gamma^{-1} \left[7.37 \times 10^{-6} \mathcal{J}_p \left(\frac{K^3}{1 + K^2} \right) \left(1 + \left(\frac{\beta_u}{\beta_{ext}} \right)^2 \right)^{\frac{1}{2}} \right]^{\frac{1}{3}}. \quad (8)$$

At this point, three regions of optimization are defined by whether $\beta_u \ll \beta_{ext}$, $\beta_u = \beta_{ext}$, or $\beta_u \gg \beta_{ext}$ [7]. For the present paper we can restrict our discussion to the last, or "weak-field" case, which leads to an optimum K value of 1, yielding

$$\rho = \left[\frac{1.17 \times 10^{-6} \mathcal{J}_p \gamma}{\beta_{ext}} \right]^{\frac{1}{3}}. \quad (9)$$

In this regime, we explicitly recognize the external focusing beta as an independent design parameter for optimizing the performance of a weak-field FEL undulator. Recent studies employing 3D FEL theory [10,13] suggest that sextupole focusing appears optimal for low energy, moderate emittance operation, while quadrupole focusing is optimal for high energy, low emittance devices. Noting that the elements for both types of focusing have been developed in the present work, we consider a FODO lattice composed of planar PM quadrupoles. For each quad, the focal length in meters is approximable by (see Fig. 1)

$$f \cong \frac{4E[\text{GeV}] \left(g^2 + 2gh \right)}{3B_r L h}, \quad (10)$$

where E is the beam energy and L is the length of the quad. With D the distance between neighboring quads in the FODO lattice, the phase advance per cell will be given by D/f radians, and we have $\beta_{ext} = 2f$. From eq. (10) and the preceding expressions, it is clear that the large practical parameter ranges of the PM quad imply a high degree of variability for both β and its (min-max) variation along the undulator axis.

Another potentially useful application would be to use successive reductions of β_{ext} to incrementally increase the ρ in a series of successive weak-field undulators, each with $K = 1$, but tuned to successively higher energies in a harmonic-generation FEL configuration [8]. This so-called technique of "p-cooling" [14], which reduces the effects of energy spread induced by preceding undulators, could be important in determining the maximum harmonic multiple that could be generated in a practical configuration.

A final issue of practical importance concerns the effects of fabrication, installation, and operating tolerances of the planar multipoles on their performance. Although a full discussion is outside the scope of this paper, it is useful to point out that simple scaling rules apply to the PM quad. Specifically, if the C_{11} coefficients of a PM quad and a conventional iron structure are equal, their positional tolerances will be identical, provided neither the beam nor the quad are subject to overly large positional shifts (which would activate the higher order field components). If the PM quad has a gradient n times larger than the conventional structure, its positional tolerance will be n times smaller. Selected issues regarding the sensitivity of field quality to mechanical and magnetic tolerances are discussed elsewhere [4,5].

6. Acknowledgments

Useful discussions with members of the SLAC Linac Coherent Light Source (LCLS) group, in particular R. Bonifacio, are acknowledged. This research was performed at SSRL and SLAC, which are operated by the Department of Energy, Offices of Basic Energy Sciences and High Energy and Nuclear Physics.

Table 1

Material, dimensional, and field parameters of PM planar multipole samples.

	<u>NdFe/B Quadrupole</u>	<u>NdFe/B Sextupole</u>
	(Sample 1)	(Sample 3)
B_r (remanent field)	1-1.2 T	1-1.2 T
Length	3 cm	3 cm
PM height	2.5 mm	5 mm
Gap	1 cm	1 cm
Width (side pieces)	1 cm	2.633 mm
Width (central pieces)	-	3.2 mm

Table 2

Calculated vs. measured field components (gradients [T/m] for the quadrupole and amplitudes [T] for the sextupole) of PM planar multipole samples.

	<u>NdFe/B Quadrupole</u> ^{a)}		<u>NdFe Sextupole</u> ^{b)}	
	(Sample 1)		(Sample 3)	
	<u>Free-space</u>	<u>Steel Plates</u>	<u>Free-space</u>	<u>Steel Plates</u>
t^*	-	2.67mm	-	0mm
Quadrupole (calc.)	57.6	65.3	-	-
Quadrupole (meas.)	57.6	64.2	-	-
Octupole (calc.)	14.4	14.5	-	-
Octupole (meas.)	14.6	14.4	-	-
Dipole (calc.)	-	-	0	0.013
Dipole (meas.)	-	-	0.0031	0.0146
Sextupole (calc.)	-	-	0.0222	0.0239
Sextupole (meas.)	-	-	0.0222	0.0237

* distance between steel plates and top and bottom PM multipole surfaces.

a) $B_r=1.2T$; b) $B_r=1.15T$

7. References

- [1] K. Halbach, "Design of Permanent Multipole Magnets with Oriented Rare Earth Cobalt Materials," Nuclear Instruments and Methods 169, 1(1980).
- [2] R. Tatchyn, R. Boyce, K. Halbach, H.-D. Nuhn, J. Seeman, H. Winick, C. Pellegrini, "Design Considerations for a 60 Meter Pure Permanent Magnet Undulator for the SLAC Linac Coherent Light Source," Proceedings of the Particle Accelerator Conference (PAC'93), Washington, D. C., May 17-20, 1993, SLAC-PUB-6106.
- [3] R. Tatchyn, "Permanent Magnet Edge-Field Quadrupoles As Compact Focussing Elements for Single-Pass Particle Accelerators," SLAC-PUB-6058.
- [4] R. Tatchyn, "Planar Permanent Magnet Multipoles for Particle Accelerator and Storage Ring Applications," submitted to IEEE Trans. Mag., 1993.
- [5] J. Cobb, R. Tatchyn, "Tests of Planar Permanent Magnet Multipole Focusing Elements," - presented at the 8th National Conference on Synchrotron Radiation Instrumentation, Gaithersburg, MD, August 23-26, 1993.
- [6] Location: 11248 Playa Court, Culver City, CA, 90230-8162.
- [7] R. Tatchyn, "Optimal Insertion Device Parameters for SASE FEL Operation," Proceedings of the Workshop on Fourth Generation Light Sources, M. Cornacchia and H. Winick, eds., SSRL Report No. 92/02, p. 605.
- [8] H. Winick, K. Bane, R. Boyce, J. Cobb, G. Loew, P. Morton, H.-D. Nuhn, J. Paterson, P. Pianetta, T. Raubenheimer, R. Tatchyn, J. Seeman, V. Vylet, C. Pellegrini, J. Rosenzweig, G. Travish, D. Prosnitz, E. T. Scharlemann, K. Halbach, K.-J. Kim, R. Schlueter, M. Xie, R. Bonifacio, L. DeSalvo, P. Pierini, "Short Wavelength FELs Using the SLAC Linac," - presented at the 8th National Conference on Synchrotron Radiation Instrumentation, Gaithersburg, MD, August 23-26, 1993.
- [9] G. A. Deis, "A Long Electromagnetic Wiggler for the PALADIN Free-Electron Laser Experiments," IEEE Trans. Mag. 24(2), 1090(1988).
- [10] E. T. Scharlemann, "Wiggle-plane focusing in linear wigglers," J. Appl. Phys. 58(6), 2154(1985).
- [11] J. B. Murphy and C. Pellegrini, "Introduction to the Physics of the Free Electron Laser," in Lecture Notes in Physics, Vol. 296, M. Month and S. Turner, eds., Springer-Verlag, Berlin, 1988, pp. 163-219.
- [12] R. Tatchyn, "Design considerations for a new weak-field soft X-ray undulator/FEL driver for PEP," Nucl. Instrum. Meth. A308, 152(1991).
- [13] G. Travish, J. Rosenzweig, "Numerical Studies of Strong Focussing in Planar Undulators," presented

at the 1993 Particle Accelerator Conference, Washington, D. C., May 17-20, 1993, presentation Mb31.

[14] R. Bonifacio, "A new approach to XUV: the ρ -cooling technique," Optics Communications 81(5), 311(1991).

DISCLAIMER

This report was prepared as an account of work sponsored by an agency of the United States Government. Neither the United States Government nor any agency thereof, nor any of their employees, makes any warranty, express or implied, or assumes any legal liability or responsibility for the accuracy, completeness, or usefulness of any information, apparatus, product, or process disclosed, or represents that its use would not infringe privately owned rights. Reference herein to any specific commercial product, process, or service by trade name, trademark, manufacturer, or otherwise does not necessarily constitute or imply its endorsement, recommendation, or favoring by the United States Government or any agency thereof. The views and opinions of authors expressed herein do not necessarily state or reflect those of the United States Government or any agency thereof.

8. Figure Captions

Figure 1. Front views of permanent magnet quadrupole (left) and sextupole (right) configurations with arbitrary parameters. The structures have length L in the z direction.

Figure 2. Experimental PM multipole samples in image-tuning geometries. For free space measurements, $t \rightarrow \infty$.

Figure 3. Rotating-coil spectra for free-space (top) and image-tuned (bottom) measurements. Field components sampled at a radius of 2mm.

Figure 4. A front view of PALADIN's yoke showing the (Sample 1) NdFe/B quadrupole installed concentrically with PALADIN's axis. In the experimental characterization of the yoke+quad fields, $g=18\text{mm}$, and the quadrupole is centered in a plane containing the maximum value of B_y .

Figure 5. Scans of $B_y(x)$ along the center of an x - y plane bisecting two opposed PALADIN poles, both with and without the installed quadrupole.

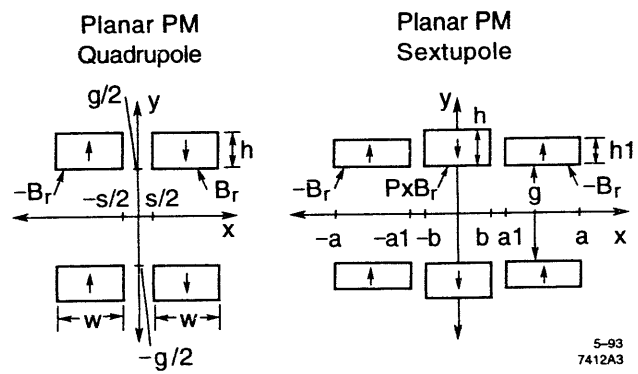
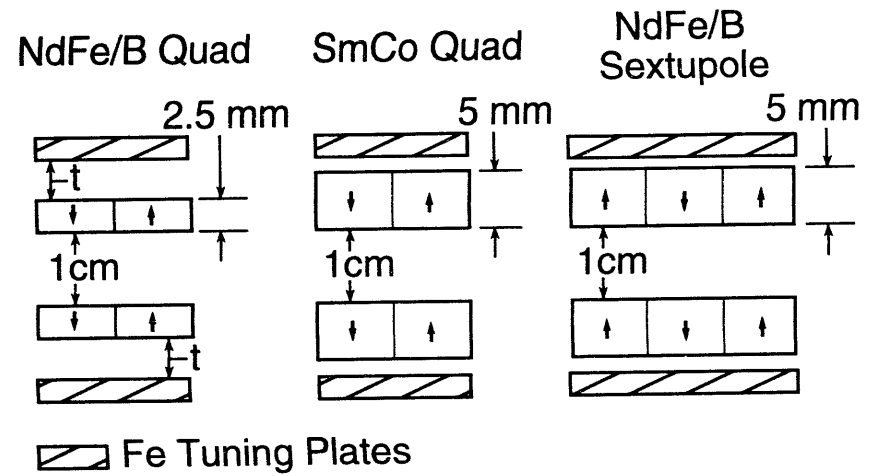


Fig. 1

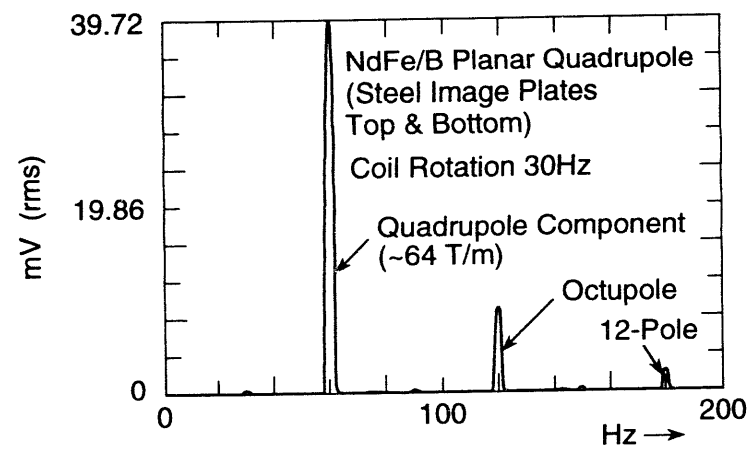
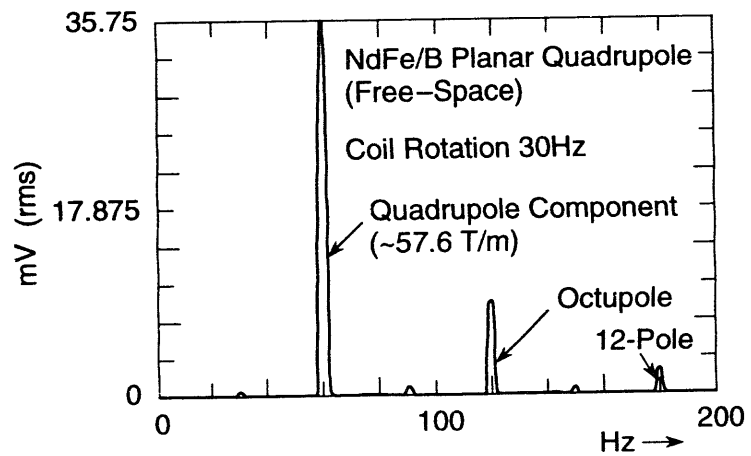
PM Planar Multipoles (Front View)



8-93

7523A4

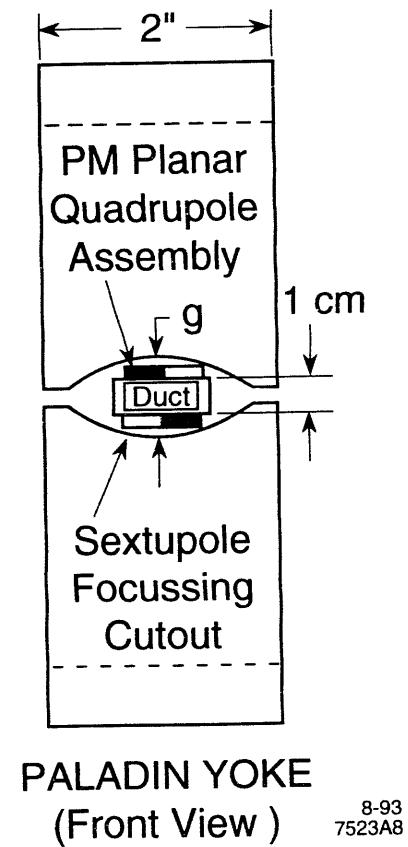
Fig. 2



8-93

7523A7

Fig. 3



8-93
7523A8

Fig. 4

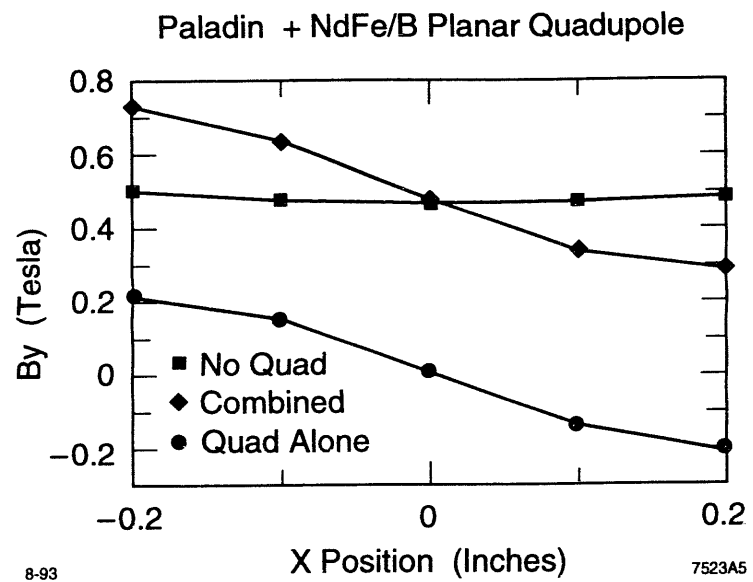


Fig. 5

DATE

FILMED

4 / 21 / 94

END

